Role and timing of GTP binding and hydrolysis during EF-G-dependent tRNA translocation on the ribosome

Berthold Wilden[†], Andreas Savelsbergh[†], Marina V. Rodnina[‡], and Wolfgang Wintermeyer[†§]

Institutes of [†]Molecular Biology and [‡]Physical Biochemistry, University of Witten-Herdecke, D-58448 Witten, Germany

Communicated by Harry F. Noller, University of California, Santa Cruz, CA, July 19, 2006 (received for review March 24, 2006)

The translocation of tRNA and mRNA through the ribosome is promoted by elongation factor G (EF-G), a GTPase that hydrolyzes GTP during the reaction. Recently, it was reported that, in contrast to previous observations, the affinity of EF-G was much weaker for GTP than for GDP and that ribosome-catalyzed GDP–GTP exchange would be required for translocation [Zavialov AV, Hauryliuk VV, Ehrenberg M (2005) *J Biol* 4:9]. We have reinvestigated GTP/GDP binding and show that EF-G binds GTP and GDP with affinities in the 20 to 40 μM range (37°C), in accordance with earlier reports. Furthermore, GDP exchange, which is extremely rapid on unbound EF-G, is retarded, rather than accelerated, on the ribosome, which, therefore, is not a nucleotide-exchange factor for EF-G. The EF-G·GDPNP complex, which is very labile, is stabilized 30,000-fold by binding to the ribosome. These findings, together with earlier kinetic results, reveal that EF-G enters the pretranslocation ribosome in the GTP-bound form and indicate that, upon ribosome-complex formation, the nucleotide-binding pocket of EF-G is closed, presumably in conjunction with GTPase activation. GTP hydrolysis is required for rapid tRNA–mRNA movement, and P_i release induces further rearrangements of both EF-G and the ribosome that are required for EF-G turnover.

fluorescence | GTP-binding protein | nucleotide exchange | transient kinetics | translation

In the translocation step of the elongation cycle, peptidyl-tRNA moves from the A site of the ribosome to the P site, carrying the mRNA along, and deacylated tRNA moves out of the P site into the E site from where it dissociates. Translocation is promoted by elongation factor G (EF-G), a large, five-domain GTPase that hydrolyzes GTP during the reaction. According to pre-steady-state kinetic analyses, EF-G binds to the pretranslocation ribosome in the GTP-bound form and subsequent rapid GTP hydrolysis precedes translocation (1, 2). Further analyses revealed that GTP hydrolysis drives a rearrangement of the ribosome, referred to as unlocking, that precedes and limits the rate of tRNA–mRNA movement (3). When GTP hydrolysis is avoided by using nonhydrolyzable GTP analogs, such as GDPNP or GDPCP (4, 5), EF-G still promotes translocation, albeit at a 50-fold lower rate (1), and the dissociation of EF-G from the ribosome is slowed down by about the same factor (6). The release of inorganic phosphate (P_i) from ribosome-bound EF-G·GDP·P_i is not required to drive translocation, because ribosomes containing mutant protein L7/12, which are slow in P_i release and in EF-G turnover, remain rapid in single-round translocation (3, 7). Thus, the driving force of EF-G action in ribosome unlocking is a conformational change that is induced by GTP hydrolysis. Subsequent P_i release induces another conformational change that is required for EF-G to dissociate from the ribosome (7). GTP hydrolysis reduces the free energy of activation of translocation by ≈2.5 kcal/mol. The difference results from a large decrease of the activation enthalpy and a small change of the entropy term, which is positive with a nonhydrolyzable GTP analog and negative with GTP (6). This finding suggests that GTP hydrolysis induces the formation of additional interactions between EF-G and the ribosome that limit the degree of conformational freedom and stabilize the complex in the unlocked state of the ribosome. Without any nucleotide, EF-G is not able to enhance translocation beyond the rate of the spontaneous reaction taking place in the absence of EF-G (1), indicating that nucleotide-free EF-G is not able to stabilize the translocation-active unlocked state of the ribosome that forms by spontaneous conformational fluctuations of the ribosome.

Recently, Zavialov *et al.* (8) have challenged the unlocking model of translocation outlined above. They reported that, in contrast to previous reports (5, 9), the affinity of EF-G for GTP was much lower (>60-fold) than that for GDP and that, at the GTP/GDP concentrations in the cell, EF-G would be present, and enter the ribosome, in the GDP-bound form, and that subsequent ribosome-catalyzed GDP–GTP exchange would promote tRNA–mRNA movement before GTP hydrolysis, and that GTP hydrolysis took place only after the movement (8). Furthermore, the authors claimed that the (slow) translocation promoted by EF-G with GDP that we have reported (1, 6) was due to GTP contaminating the GDP preparation we have used. These claims have prompted us to reinvestigate GDP/GTP binding to EF-G, to measure the kinetics of GDP-GTP exchange on free and ribosome-bound EF-G, and to redetermine the kinetics of translocation with purified GTP and GDP. Our results do not confirm the results of Zavialov *et al.* (8) and fully support our previous conclusions. In a more general sense, this result emphasizes the importance of using the pre-steady-state, rather than steady-state, approach and of studying steps of interest in the appropriate time range to obtain mechanistic information on a process as complex as translocation.

Results

Affinities of GDP/GTP Binding to EF-G. Binding of GDP and GTP to *Escherichia coli* EF-G was studied at equilibrium by fluorescence titrations carried out in different ways. In the first set of experiments, titrations were carried out with the (2′,3′)-*O*-(*N*-methylanthraniloyl) (mant) derivatives of GDP and GTP. The fluorescence of the mant group was excited by fluorescence resonance energy transfer (FRET) from tryptophan residues located in the vicinity of the nucleotide-binding pocket in the G domain of EF-G (see *Materials and Methods*). Increasing amounts of mant-labeled nucleotides were added to a fixed amount of EF-G, or to buffer without EF-G, and the difference between the fluorescence signals measured in the presence and absence of EF-G was plotted against the nucleotide concentration (Fig. 1*A*). Evaluation of the titration curves by fitting a quadratic equation (see *Materials and Methods*) yielded K_d values of 17 and 7 μM for mant-GDP and mant-GTP, respectively.

The purity of the mant nucleotides was checked by TLC (Fig. 1*B*). The analysis revealed that mant-GDP did not contain a detectable amount of mant-GTP, setting the contamination level to <0.1%, whereas mant-GTP contained a trace amount (≈1%)

Conflict of interest statement: No conflicts declared.

Abbreviations: EF-G, elongation factor G; mant, (2′,3′)-*O*-(*N*-methylanthraniloyl).

[§]To whom correspondence should be addressed. E-mail: winterme@uni-wh.de.

www.pnas.org/cgi/doi/10.1073/pnas.0606099103

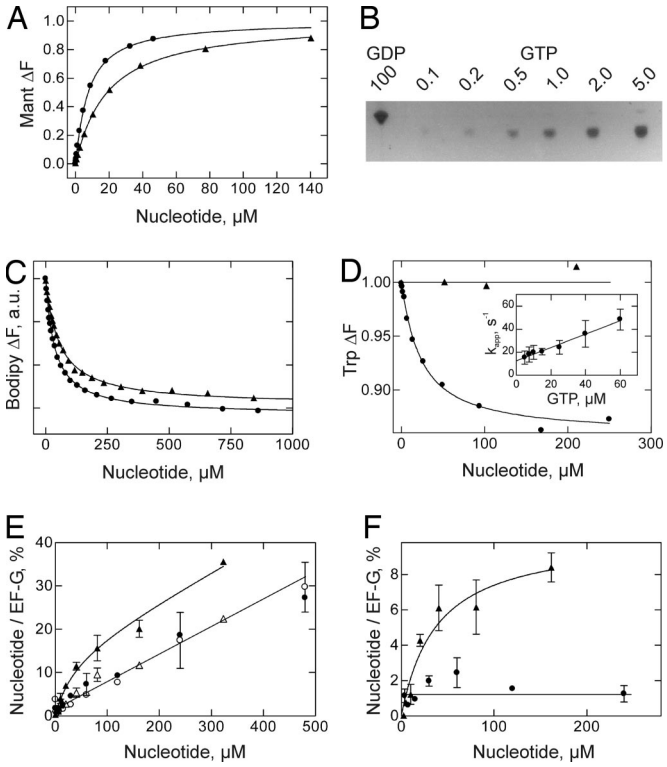

Fig. 1. GTP/GDP binding to EF-G. (*A*) Fluorescence titrations with mant-GTP (circles) and mant-GDP (triangles). (*B*) TLC of mant-GTP and mant-GDP. (*C*) Chase titrations with GTP (circles) or GDP (triangles) monitoring the fluorescence of Bodipy FL-GDP. (*D*) Titrations monitoring tryptophan fluorescence. GTP (circles) or GDP (triangles). (*Inset*) Concentration dependence of GTP binding kinetics. $k_{on} = 0.58 \pm 0.04\ \mu M^{-1} \cdot s^{-1}$; $k_{off} = 13 \pm 1\ s^{-1}$. (*E*) Binding of [^{3}H]GDP (triangles) or [^{3}H]GTP (circles) to nitrocellulose filters in the presence (filled symbols) or absence (open symbols) of EF-G. (*F*) Retention of EF-G·[^{3}H]GDP (triangles) and EF-G·[^{3}H]GTP (circles) on nitrocellulose filters. Shown are difference titration curves from *E*. In *A–D*, continuous lines represent fits (see *Materials and Methods*).

of mant-GDP. The affinities of unmodified GDP and GTP, purified by HPLC as described in ref. 8 and *Materials and Methods*, were determined by competition fluorescence titrations, monitoring the fluorescence of Bodipy-GDP (Fig. 1*C*), which yielded K_d values of 40 and 25 μM, respectively.

Finally, the binding of GTP to EF-G could also be measured by tryptophan fluorescence, which is quenched by GTP but not by GDP (Fig. 1*D*). The K_d value resulting from the titration was 20 μM. The same value (22 μM) was obtained from k_{on} and k_{off} values determined by stopped-flow kinetics, monitoring tryptophan fluorescence (Fig. 1*D Inset*).

These results are consistent with the early literature (9, 10), which reported affinities of EF-G binding for GDP and GTP in the 10 to 20 μM range (4°C). A similar value for GDP, 10 μM, and a much lower value for GTP, >600 μM, has been reported by Zavialov *et al.* (8), based on nitrocellulose filtration data. However, because the kinetic stability of the complexes is low, the filtration technique is not suitable for studying nucleotide binding to EF-G. This is evident from filtration experiments with ^{3}H-labeled nucleotides (Fig. 1*E*). With [^{3}H]GTP, the titration curves obtained with and without EF-G were indistinguishable, indicating that [^{3}H]GTP was not retained on filter-bound EF-G. With [^{3}H]GDP, a small amount was retained, but the saturation level remained below 10% of the EF-G present (Fig. 1*F*), as in the experiments of Zavialov *et al.* (8), precluding any reliable conclusion.

For comparison, the affinities for GTP/GDP were also measured for EF-G from *Thermus thermophilus* and *Thermotoga*

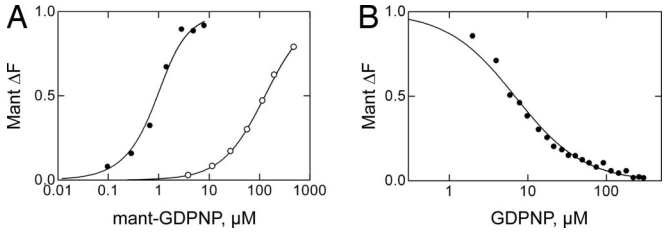

Fig. 2. Equilibrium binding of GDPNP to free and ribosome-bound EF-G. (*A*) mant-GDPNP. Free EF-G (open symbols) and ribosome-bound EF-G (filled symbols) were titrated with mant-GDPNP as in Fig. 1*A*. Control titrations without EF-G showed no signal change. Apparent K_d values: Free EF-G, 120 μM; ribosome-bound EF-G, 0.5 μM. (*B*) GDPNP. Mant-GDPNP was chased from ribosome-bound EF-G by adding increasing amounts of GDPNP. Apparent K_d = 2 μM. Continuous lines represent fits (see *Materials and Methods*); standard deviations of K_d values were ±20%.

maritima. Competition titrations monitored by the fluorescence of Bodipy-GDP (cf. Fig. 1*C*) yielded K_d values (37°C) for GTP and GDP of 5 μM for *Thermus thermophilus* EF-G and of 20 and 4 μM, respectively, for *Thermotoga maritima* EF-G (data not shown). For *Thermus thermophilus* EF-G, values of 0.6 to 0.9 μM for GDP and 12 to 14 μM for GTP (4°C) were obtained previously, using nitrocellulose filtration at somewhat different buffer conditions (11, 12).

To obtain an estimate for the affinity of GTP to ribosome-bound *E. coli* EF-G, which cannot be determined directly because of rapid GTP hydrolysis (1, 2), we have performed titrations with mant-GDPNP (Fig. 2*A*). Free EF-G bound mant-GDPNP rather weakly, with a K_d of 130 μM, about six times less strongly than mant-GTP, whereas in the presence of ribosomes, the binding was much stronger (apparent K_d = 0.5 μM). Formally, the apparent K_d reflects at least two equilibria that lead to the formation of the ternary ribosome·EF-G·GTP complex; because the titration was performed at saturating concentration of ribosomes (2 μM), the K_d reflects nucleotide binding to ribosome-bound EF-G. The competition titration with unlabeled GDPNP yielded an apparent K_d of 2.1 μM for the ribosome·EF-G·GDPNP complex (Fig. 2*B*), indicating a slight affinity loss due to the absence of the mant group, in line with the results obtained with GDP and GTP. With the assumption that the 6-fold affinity difference between GTP and GDPNP in binding to free EF-G also applies to ribosome-bound EF-G, the apparent K_d of the ribosome·EF-G·GTP complex is estimated to be 0.3 μM. Comparable values (determined at 4°C) were previously reported for GDP (0.1 μM) and GDPCP (0.06 μM) (9), indicating that on the ribosome, the affinity of EF-G for both GTP and GDP is strongly increased. An affinity of the ribosome·EF-G·GTP complex of ≈0.1 to 0.3 μM is consistent with K_M values for EF-G close to 0.1 μM, as determined by measuring initial rates of GTP hydrolysis or translocation under conditions of EF-G turnover (7).

Dissociation of Guanine Nucleotides from Free and Ribosome-Bound EF-G. Based on their nucleotide binding data, Zavialov *et al.* (8) inferred that EF-G entered the ribosome in the GDP-bound form and that the ribosome catalyzed the exchange of GDP for GTP on EF-G, although they did not examine nucleotide exchange directly. We have measured the kinetics of GDP dissociation from free and ribosome-bound EF-G, using fluorescent mant-GDP. The dissociation of mant-GDP was initiated by mixing with a large excess of unlabeled GDP (unlabeled GTP yielded identical results; data not shown) without or with ribosomes (Fig. 3). The dissociation of mant-GDP from unbound EF-G was extremely rapid with a rate constant of ≈300 s^{-1} (Fig. 3, trace 1), whereas in the presence of ribosomes, the dissociation was slowed down ≈30-fold, to ≈10 s^{-1}

BIOCHEMISTRY

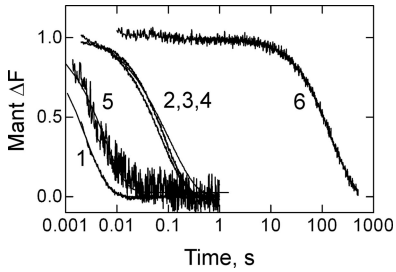

Fig. 3. Dissociation of mant-labeled nucleotides from free and ribosome-bound EF-G. The dissociation of mant-GDP (traces 1 and 2), mant-GTP (traces 3 and 4), and mant-GDPNP (traces 5 and 6) from free EF-G (traces 1, 3, and 5) or ribosome-bound EF-G (traces 2, 4, and 6) as induced by rapid mixing with excess unlabeled GDP (traces 1–4) or GDPNP (traces 5 and 6) was monitored by fluorescence. Dissociation rate constants are summarized in Table 1. For details, see *Materials and Methods*.

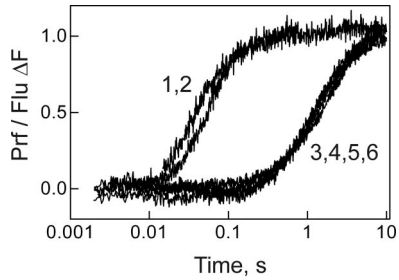

Fig. 4. Translocation with GTP, GDP, and GDPNP. Time courses of translocation were measured by fluorescence stopped-flow, monitoring the fluorescence of proflavin-labeled fMetPhe-tRNA^{Phe} (traces 1, 4, and 6) or of mRNA(fluorescein + 14) (traces 2, 3, and 5). Time courses were evaluated by single-exponential fitting (see *Materials and Methods*) to obtain the following values for k_{app} (SD ±15%): trace 1, GTP, 21 s^{-1}; trace 2, GTP, 18 s^{-1}; trace 3, GDPNP, 0.8 s^{-1}; traces 4 and 5, GDP, 0.9 s^{-1}; trace 6, mant-GDP, 0.6 s^{-1}.

(trace 2). The dissociation of mant-GTP from EF-G took place with a rate constant of 7 s^{-1} (Fig. 3, trace 3), and about the same rate (10 s^{-1}) was observed in the presence of ribosomes (Fig. 3, trace 4). However, the latter value represented the dissociation of mant-GDP, rather than that of mant-GTP, because of rapid hydrolysis of mant-GTP by EF-G on the ribosome (>100 s^{-1} at the concentrations used here).

To obtain an estimate for GTP, we have measured the rates of the dissociation of nonhydrolyzable mant-GDPNP from free and ribosome-bound EF-G. The effect of ribosome binding was found to be very large: whereas mant-GDPNP dissociated from free EF-G with a rate constant of ≈200 s^{-1} (Fig. 3, trace 5), the dissociation from ribosome-bound EF-G was very slow, ≈0.006 s^{-1} (Fig. 3, trace 6), indicating that on the ribosome, mant-GDPNP binding was stabilized ≈30,000 times. Taking into account the slight stabilizing effect of the mant group (see above), the dissociation rate constant of unmodified GDPNP is estimated to be ≈0.02 s^{-1}. These results indicate that nucleotide binding to EF-G is stabilized considerably when EF-G is bound to the ribosome, presumably by closing the nucleotide-binding pocket. This finding is in direct contrast to the model of Zavialov *et al.* (8), in which the ribosome acts as a nucleotide-exchange factor for EF-G, implying that it destabilized, rather than stabilized, GDP binding.

The dissociation of mant-GDP from ribosome-bound EF-G was not systematically influenced by the functional state of the ribosome, because dissociation rate constants between 6 and 20 s^{-1} were obtained for different complexes (Table 1). These rates are higher than the rate of EF-G turnover, k_{cat}, which was ≈3 s^{-1} for these complexes or for vacant ribosomes (ref. 7 and data not shown). This finding indicates that, after unlocking and further rearrangements induced by P_i release, GDP can dissociate before EF-G dissociates from the ribosome.

Translocation with GDP. When GTP is replaced with nonhydrolyzable GTP analogs, translocation is slowed down >50-fold, to ≈0.5 s^{-1} (1, 6). The same slow rate we have previously observed with GDP (1). Enthalpies and entropies of activation with GDP and GTP were quite different, indicating that different steps were rate-limiting (6). Recently, Zavialov *et al.* (8) suggested that translocation with GDP was to be attributed to a GTP contamination, because they were not able to see translocation with purified GDP. We have remeasured the kinetics of translocation using fluorescent peptidyl-tRNA (6) and GDP purified by their procedure; the results (Fig. 4) confirmed our previous results, i.e., rapid translocation with GTP and slow, but substantial, translocation with GDP at a rate, 0.9 s^{-1}, comparable with the rate we observed previously. With purified mant-GDP (see Fig. 1*B* for proof of purity), translocation at a similar rate, 0.6 s^{-1}, was observed. The same results were obtained when translocation was monitored by the signal of a fluorescent mRNA derivative (13). Importantly, the latter assay, which directly monitors mRNA movement on the 30S subunit, also showed that translocation is slow, ≈0.8 s^{-1}, when GDPNP is used, confirming our previous results (6). Thus, the present results are fully consistent with our previous observations, i.e., that EF-G-stimulated translocation proceeds at about the same rate in the presence of GDP as in the presence of nonhydrolyzable GTP analogs and that GTP hydrolysis is required for rapid translocation to take place.

Discussion

In line with the majority of the literature, the present results, which were obtained by direct or indirect fluorescence titrations

Table 1. Rate constants of nucleotide dissociation from free and ribosome-bound EF-G (37°C)

			k_{off}, s^{-1}		
Ribosome	P site tRNA	A site tRNA	mant-GDP	mant-GTP	mant-GDPNP
—			300	7	200
Vacant	—	—	10	(10)†	0.006
Pretrans‡	Deacyl	Peptidyl	6	ND	ND
Posttrans§	Peptidyl	—	20	ND	ND
Postterm¶	Deacyl	—	14	ND	ND

Standard deviations of rate constants were ±15% or less (see *Materials and Methods*). ND, not determined; —, none.

†Dissociation of mant-GDP due to rapid hydrolysis of mant-GTP on the ribosome.

‡Pretranslocation complex stabilized by viomycin (0.1 mM).

§Posttranslocation complex.

¶Posttermination complex obtained by treating posttranslocation complex with puromycin (1 mM, 1 min, 37°C).

at equilibrium, show that EF-G has similar affinities for GDP and GTP of ≈40 and 20 μM (37°C), respectively. These K_d values are in the same range as those reported previously by Kaziro and coworkers (5), 11 and 14 μM (4°C), and by Baca *et al.* (9), 4 and 40 μM (4°C), although our results indicate that GTP has a slightly higher affinity than GDP. Zavialov *et al.* (8) have reported a similar value for GDP, 10 μM, whereas their estimate for GTP was extremely high, >600 μM. Previous (5, 9) and our present results (Fig. 1) clearly show that this high K_d value for GTP is due to the nitrocellulose filtration technique used to quantify the EF-G·GTP complex, which is inadequate because the complex is unstable and dissociates rapidly (Fig. 3). In line with previous reports, we observed that ribosome binding considerably increased the affinity of EF-G for both GDP and GTP binding, indicated by apparent K_d values of 0.1 to 0.3 μM for the ternary ribosome·EF-G·nucleotide complex. In both cases, the affinity increase is, at least in part, explained by decreased dissociation rate constants, which in the case of GTP (measured with mant-GDPNP) was decreased ≈30,000-fold. The stabilization of nucleotide binding to EF-G on the ribosome is inconsistent with a model where the ribosome acts as a nucleotide-exchange factor for EF-G (8). In fact, GDP dissociation from free EF-G is extremely rapid, ensuring that under the conditions prevailing in the cell, where the concentration of GTP is about 10 times higher than that of GDP, most of the EF-G is present, and will enter the ribosome, in the GTP-bound form. A small fraction of EF-G may bind to the ribosome in the GDP-bound form; however, despite the stabilization of nucleotide binding on the ribosome, the dissociation of GDP or EF-G·GDP remains rapid enough (10 s^{-1}) to allow for the binding of GTP or EF-G·GTP, i.e., the formation of the translocation-active ribosome·EF-G·GTP complex, in a reasonable time range.

The translocation model of Zavialov *et al.* (8) proposes that the exchange of GDP from ribosome-bound EF-G·GDP (referred to as "pre-T* state") with GTP induced tRNA–mRNA movement, without GTP hydrolysis, to reach a trans-T* state, and that GTP hydrolysis would take place only after tRNA movement to reverse the conformational change of the ribosome induced by initial EF-G binding, forming the post-T state. However, kinetic data were not presented, rendering the conclusions as to the timing of tRNA–mRNA movement and GTP hydrolysis questionable. In fact, the model of Zavialov *et al.* (8) does not take into account previous kinetic results which show that GTP hydrolysis is much more rapid (rate constant of ≈200 s^{-1}; 37°C) (1–3, 7, 14) than, and therefore must precede, tRNA–mRNA movement (≈30 s^{-1}) (1, 13, 15, 16) and that the movement is much slower (≈0.5 s^{-1}) when nonhydrolyzable GTP analogs (1, 6) or GTPase-inactive EF-G mutants (17) are used. These kinetic results have established a sequence of steps in translocation that is fundamentally different from that proposed by Zavialov *et al.* (8) on the basis of steady-state data alone. The problem with the interpretation of the steady-state data is that translocation without GTP hydrolysis, e.g., in the presence of a nonhydrolyzable GTP analog, at a rate of ≈0.5 s^{-1} is still fast enough to be completed within the incubation times (minutes) of biochemical translocation assays, suggesting that tRNA–mRNA movement was independent of GTP hydrolysis, which it is not. To understand the mechanism of how EF-G accelerates translocation to a rate that is relevant for protein synthesis *in vivo*, i.e., >10 s^{-1}, the reaction has to be studied in the relevant time range by using rapid kinetic techniques.

According to the kinetic data, the binding of EF-G·GTP to the ribosome induces a conformational change of EF-G (GTPase activation) that leads to rapid GTP hydrolysis, resulting in EF-G·GDP·P_i. The GTPase activation rearrangement may be related to the rearrangement of an initial ribosome·EF-G·GDPCP complex reported recently (2). P_i remains bound to EF-G until the unlocking step has taken place (3), indicating that the nucleotide-binding pocket is closed, presumably in conjunction with GTPase activation, in keeping with the strong stabilization and the increase of the apparent affinity of GTP binding to EF-G on the ribosome. Thus, the free energy of GTP hydrolysis is not dissipated but used for bringing about another conformational change of EF-G that is coupled to the unlocking rearrangement of the ribosome, which presumably leads to changes of the interactions between the ribosomal subunits. These changes, in turn, allow the movement of the tRNAs together with the mRNA and, in parallel, the release of P_i and, somewhat more slowly, of GDP, implying that during unlocking, the nucleotide-binding pocket of EF-G is opened. It is not clear how the unlocking rearrangement of the ribosome, as deduced from kinetics, is related to the "ratcheting" movement of the ribosomal subunits relative to one another that, according to cryo-EM, is induced by the binding of EF-G with the nonhydrolyzable GTP analog GDPCP (18, 19), i.e., without GTP hydrolysis (20). Based on cryo-EM evidence, the tRNA movement is accompanied by a repositioning of EF-G during which domain 4 moves from a position where it touches the shoulder of the 30S subunit into a position where it occupies the 30S A site vacated by the movement of the tRNA (21).

The unlocking model implies that EF-G before GTP hydrolysis establishes strong interactions with the ribosome, because conformational coupling otherwise would not be effective. This contention is in keeping with the observed high kinetic stability of the ribosome complexes with EF-G·GTP (measured with GDPNP), which is 30,000 times more stable than the EF-G·GTP complex off the ribosome. The release of the interactions between EF-G and the ribosome and the dissociation of EF-G requires another conformational change of EF-G, and probably of the ribosome as well, which is induced by the dissociation of P_i from EF-G·GDP·P_i (7).

Translocation by EF-G with GDP at first sight seems paradoxical, as GDP is one of the products of GTP-driven translocation that dissociates from ribosome-bound EF-G at the end of the functional cycle. The rate of translocation observed with EF-G in the presence of GDP, 0.5–1 s^{-1}, is the same as that observed with nonhydrolyzable GTP analogs or with GTPase-inactive mutants of EF-G (6, 17). These results are readily explained by assuming that the formation of the unlocked state of the ribosome without GTP hydrolysis is not driven by the conformational change of EF-G but is reached by thermal fluctuations. By establishing interactions with the ribosome, EF-G traps conformational states of the ribosome that form spontaneously and facilitate tRNA movement. Nucleotide-free EF-G does not promote translocation (1), presumably because its conformation is too flexible to be able to restrict conformational fluctuations of the ribosome toward the translocation state. Thus, any guanine nucleotide bound to EF-G seems to stabilize a more rigid conformation of the factor that is able to trap the unlocked, translocation-active conformation of the ribosome. Without additional energy input from GTP hydrolysis, the dissolution of the interactions between the ribosome and EF-G is unfavorable, hence the relatively slow dissociation of EF-G from the ribosome when GTP is replaced with nonhydrolyzable analogs (4–6) or GDP (1, 6).

The unlocking model of EF-G function involves at least four different conformations of EF-G, which are assigned to biochemically defined intermediates of translocation: (*i*) the GTP-bound conformation in which EF-G is present in the unbound state and enters the ribosome; (*ii*) the GTPase-activated conformation that is induced upon binding to the ribosome; (*iii*) the GDP·P_i conformation that forms upon GTP hydrolysis and, by conformational coupling with the ribosome, drives the unlocking rearrangement; and (*iv*) the GDP-bound conformation that forms upon P_i release and allows for the dissociation of EF-G from the ribosome. Crystal structures are very similar for the GTP- and GDP-bound forms of EF-G (12, 22–26). For ribosome-bound EF-G, cryo-EM has re-

vealed different domain arrangements of EF-G in the states immediately before unlocking or after P_i release, which were stabilized by thiostrepton or fusidic acid, respectively, or by using nonhydrolyzable GTP analogs (19, 21, 25–28). According to these reconstructions, the major difference between those two states is a relocation of domains 4 and 5, and perhaps 3, relative to domains 1 and 2. Another conformational change of EF-G that appears to be important for tRNA movement, but not unlocking, involves a movement of domain 5 relative to domain 1, as revealed by introducing a disulfide bridge between the two domains that abrogates tRNA movement and EF-G turnover without affecting P_i release (29). More detailed structural information is required to resolve structural changes within domains of EF-G, e.g., in the switch I and II regions in the G domain, that probably are instrumental in transmitting changes taking place at the nucleotide-binding site, as induced by either GTP hydrolysis or P_i release, to other regions of the EF-G molecule.

Materials and Methods

Materials. Mant-labeled GDP, GTP, and GDPNP were purchased from Jena Bioscience (Jena, Germany). Bodipy FL-GDP was purchased from Molecular Probes (Leiden, The Netherlands). All other chemicals were purchased from Merck (Darmstadt, Germany). All experiments were performed in buffer A (50 mM Tris·HCl, pH 7.5/70 mM NH_4Cl/30 mM KCl/7 mM $MgCl_2$) at 37°C. EF-G (30) and ribosomes (31) were prepared from *E. coli* MRE600 as described.

GDP was purified on Mono Q (50 × 7 mm; Amersham Pharmacia Biotech, Munich, Germany) (8). GDP was applied in 50 mM Tris·HCl (pH 7.5), and elution was performed with a 10-ml linear gradient of KCl from 0 to 170 mM in the same buffer, followed by 20 ml of high-salt buffer. GMP, GDP, and GTP eluted from the column at 6, 10, and 13–15 min, respectively.

For analysis of purity, ≈10 nmol of mant-GDP and varying amounts of mant-GTP were spotted onto TLC plates (silica gel 60 F254; Merck). TLC plates were developed in a mixture of 2-propanol, 25% ammonium hydroxide, and water, 9:5:1 (vol/vol/vol).

Equilibrium Titrations. Dissociation constants, K_d, were determined by titrating a fixed amount of EF-G (2 μM) with labeled or unlabeled GTP or GDP. Fluorescence was measured on a PTI500 fluorimeter (Photon Technology International, Birmingham, NJ). The fluorescence of mant-GTP/mant-GDP was excited by FRET from tryptophan residues in the vicinity of the nucleotide-binding pocket in the G domain. The excitation wavelength was 290 nm, and the fluorescence of the mant group was measured at 445 nm. Blank titrations with mant-GTP/mant-GDP were performed without EF-G and were subtracted from the respective titration curves obtained in the presence of EF-G, and the difference curves (Fig. 1) were evaluated by using the following equation: $\Delta F = 0.5 \times B_{max}/P \times (K_d + P + X - \mathrm{sqrt}((K_d + P + X)^2 - 4 \times P \times X)$, where B_{max} is the amplitude, P is the total concentration of EF-G, X is the total concentration of nucleotide, and K_d is the dissociation constant. The binding of unlabeled GTP to EF-G was monitored directly by the quenching of the tryptophan fluorescence caused by GTP binding. Tryptophan residues in EF-G (5 μM) were excited at 290 nm, and the fluorescence was measured at 335 nm. Titration curves were evaluated as above. Standard deviations of K_d values were ±20%.

Chase titrations were performed by measuring the fluorescence of a solution of EF-G (3 μM) and Bodipy FL-GDP (18 μM) upon addition of GTP or purified GDP. Control titrations were performed without EF-G and were subtracted from the curve measured in the presence of EF-G; the difference curve was evaluated by the following equation: $\Delta F = F_{end} + B_{max} \times nuc^{labeled}/(nuc^{labeled} + K_d^{labeled} \times (1 + X/K_d^{unlabeled}))$, where F_{end} denotes the signal at saturation, B_{max} is the amplitude of the fluorescence change, $nuc^{labeled}$ is the total concentration of the Bodipy FL-GDP, $K_d^{labeled}$ is the dissociation constant of the Bodipy FL-GDP·EF-G complex (60 μM, data not shown), X is the concentration of the unlabeled nucleotide, and $K_d^{unlabeled}$ is the dissociation constant of the unlabeled nucleotide. Standard deviations of K_d values were ±20%.

Nitrocellulose Filtration. EF-G (1 μM) and [^{3}H]GDP (30,500 dpm/pmol), added in increasing amounts, were incubated at 37°C for 15 min. Samples were filtered through cellulose nitrate filters (Sartorius, Göttingen, Germany; 0.45 μm), and the filters were washed with 5 ml of ice-cold buffer. Filters were dissolved in a scintillation mixture (Zinsser Analytic, Berkshire, U.K.) and counted (2500TR; Packard, Rodgau-Jügesheim, Germany). Control titrations were performed without EF-G. Titrations with [^{3}H]GTP (9,900 dpm/pmol) were performed in the same way, except that [^{3}H]GTP was treated with 3 mM PEP and 50 μg/ml pyruvate kinase for 15 min at 37°C before the titration.

Kinetics of Nucleotide Binding and Dissociation. The kinetics of dissociation of mant-GTP/mant-GDP from EF-G was measured by fluorescence stopped-flow, performed on a stopped-flow apparatus (SX-18MV; Applied Photophysics, Surrey, U.K.). The fluorescence of mant-labeled nucleotides was excited at 290 nm by FRET from tryptophan residues of EF-G and measured after passing a cut-off filter (KV 408; Schott, Mainz, Germany). EF-G (1 μM, final concentrations after mixing are given throughout) was preincubated with mant-GTP (3.5 μM), mant-GDP (8.5 μM), or mant-GDPNP (25 μM) and rapidly mixed with a solution containing unlabeled GTP (1.2 mM) or GDP (2.5 mM). When ribosome·EF-G complexes were studied, EF-G (1 μM) was incubated with ribosomes or ribosome complexes (1.5 μM) in the presence of mant-GDP or mant-GDPNP (5 μM) before mixing with unlabeled GDP or GDPNP (1.2 mM). Time courses shown are averages of six to nine individual traces. Standard deviations of k_{app} values were ±15% or less.

Stopped-flow measurements of GTP binding to EF-G were monitored by tryptophan fluorescence and were performed as described above by rapidly mixing EF-G (1 μM after mixing) with GTP (3–60 μM). Values of k_{app} were determined by single-exponential fitting, and the rate constants of GTP binding, k_{on}, and dissociation, k_{off}, were determined from the slope and intercept of the linear concentration dependence of k_{app}.

Translocation Kinetics. Initiation complex was formed by incubating ribosomes with f[^{3}H]Met-tRNA^{fMet} and MFTI-mRNA (coding for Met-Phe-Thr-Ile) in buffer A with 20 mM $MgCl_2$ for 60 min at 37°C. The ternary complex, EF-Tu·GTP·[^{14}C]Phe-tRNA^{Phe}(proflavin 16/17), was prepared and purified by gel filtration as described in refs. 32 and 33. The pretranslocation complex was formed by incubating initiation complex in 1.5-fold excess over ternary complex for 1 min at 37°C; then, the Mg^{2+} concentration was adjusted to 7 mM. More than 95% of the ribosomes formed pretranslocation complex with fMetPhe-tRNA^{Phe}(proflavin 16/17) in the A site. Alternatively, pretranslocation complexes were formed on fluorescein-labeled MFTI-mRNA(fluorescein + 14) with unlabeled fMetPhe-tRNA^{Phe} in the A site, and translocation was monitored by the fluorescence of fluorescein (13). Translocation was induced by rapidly mixing pretranslocation complex (concentration after mixing, 0.2 μM) with EF-G (1 μM) and the indicated nucleotide (50 μM). The fluorescence of proflavin or fluorescein was excited at 470 nm and measured after passing a cut-off filter (KV 500; Schott). Time courses were evaluated by exponential fitting; standard deviations of k_{app} values were ±15%.

We thank Yuri Semenkov and Vladimir Katunin for generous gifts of tRNAs and Carmen Schillings, Astrid Böhm, Simone Möbitz, and Petra Striebeck for expert technical assistance. This work was supported by the Deutsche Forschungsgemeinschaft, the Alfried Krupp von Bohlen und Halbach-Stiftung, and the Fonds der Chemischen Industrie.

1. Rodnina MV, Savelsbergh A, Katunin VI, Wintermeyer W (1997) *Nature* 385:37–41.
2. Seo HS, Abedin S, Kamp D, Wilson DN, Nierhaus KH, Cooperman BS (2006) *Biochemistry* 45:2504–2514.
3. Savelsbergh A, Katunin VI, Mohr D, Peske F, Rodnina MV, Wintermeyer W (2003) *Mol Cell* 11:1517–1523.
4. Spirin, AS (1985) *Prog Nucleic Acid Res Mol Biol* 32:75–114.
5. Kaziro, Y (1978) *Biochim Biophys Acta* 505:95–127.
6. Katunin VI, Savelsbergh A, Rodnina MV, Wintermeyer W (2002) *Biochemistry* 41:12806–12812.
7. Savelsbergh A, Mohr D, Kothe U, Wintermeyer W, Rodnina MV (2005) *EMBO J* 24:4316–4323.
8. Zavialov AV, Hauryliuk VV, Ehrenberg M (2005) *J Biol* 4:9.
9. Baca OG, Rohrbach MS, Bodley JW (1976) *Biochemistry* 15:4570–4574.
10. Arai N, Arai K, Kaziro Y (1977) *J Biochem (Tokyo)* 82:687–694.
11. Arai K, Arai N, Nakamura S, Oshima T, Kaziro Y (1978) *Eur J Biochem* 92:521–531.
12. Czworkowski J, Moore PB (1997) *Biochemistry* 36:10327–10334.
13. Peske F, Savelsbergh A, Katunin VI, Rodnina MV, Wintermeyer W (2004) *J Mol Biol* 343:1183–1194.
14. Seo HS, Kiel M, Pan D, Raj VS, Kaji A, Cooperman BS (2004) *Biochemistry* 43:12728–12740.
15. Studer SM, Feinberg JS, Joseph S (2003) *J Mol Biol* 327:369–381.
16. Dorner S, Brunelle JL, Sharma D, Green R (2006) *Nat Struct Mol Biol* 13:234–241.
17. Mohr D, Wintermeyer W, Rodnina MV (2000) *EMBO J* 19:3458–3464.
18. Agrawal RK, Heagle AB, Penczek P, Grassucci RA, Frank J (1999) *Nat Struct Biol* 6:643–647.
19. Frank J, Agrawal RK (2000) *Nature* 406:318–322.
20. Valle M, Zavialov A, Sengupta J, Rawat U, Ehrenberg M, Frank J (2003) *Cell* 114:123–134.
21. Stark H, Rodnina MV, Wieden H-J, van Heel M, Wintermeyer W (2000) *Cell* 100:301–309.
22. Laurberg M, Kristensen O, Martemyanov K, Gudkov AT, Nagaev I, Hughes D, Liljas A (2000) *J Mol Biol* 303:593–603.
23. Czworkowski J, Wang J, Steitz TA, Moore PB (1994) *EMBO J* 13:3661–3668.
24. Al-Karadaghi S, Ævarsson A, Garber M, Zheltonosova J, Liljas A (1996) *Structure (London)* 4:555–565.
25. Hansson S, Singh R, Gudkov AT, Liljas A, Logan DT (2005) *FEBS Lett* 579:4492–4497.
26. Hansson S, Singh R, Gudkov AT, Liljas A, Logan DT (2005) *J Mol Biol* 348:939–949.
27. Agrawal RK, Penczek P, Grassucci RA, Frank J (1998) *Proc Natl Acad Sci USA* 95:6134–6138.
28. Agrawal RK, Spahn CM, Penczek P, Grassucci RA, Nierhaus KH, Frank J (2000) *J Cell Biol* 150:447–460.
29. Peske F, Matassova NB, Savelsbergh A, Rodnina MV, Wintermeyer W (2000) *Mol Cell* 6:501–505.
30. Rodnina MV, Savelsbergh A, Matassova NB, Katunin VI, Semenkov YP, Wintermeyer W (1999) *Proc Natl Acad Sci USA* 96:9586–9590.
31. Rodnina MV, Wintermeyer W (1995) *Proc Natl Acad Sci USA* 92:1945–1949.
32. Pape T, Wintermeyer W, Rodnina MV (1998) *EMBO J* 17:7490–7497.
33. Rodnina MV, Fricke R, Wintermeyer W (1994) *Biochemistry* 33:12267–12275.